Land Subsidence and Cracking Due to Ground-Water Depletion[a]

by Herman Bouwer[b]

ABSTRACT

Subsidence of the land surface due to ground-water overdraft is caused by an increase in the intergranular pressure in unconsolidated aquifers and other underground materials. For unconfined aquifers, this increase is the result of a loss of buoyancy of solid particles in the zone dewatered by the falling water table. For confined aquifers, increases in intergranular pressure are caused by decreases in the upward hydraulic pressure against the bottom of the upper confining layer, due to a drop in piezometric surface. Compression of layers in which the intergranular pressure is increased can be calculated with elastic or logarithmic theory. Sample calculations yield rates of subsidence that agree with those observed, i.e., about 5 to 50 cm (2 to 20 inches) per 10-m (33-ft) drop in ground-water level. Ground-water depletion can also produce surface cracks, particularly above discontinuities in bedrock depth along the periphery or in other parts of subsiding basins. Calculations based on the rotating-slab theory show that the initial surface width of such cracks is about 1 cm (0.5 inch), which agrees with field observations.

INTRODUCTION

Downward movement or subsidence of the land surface is an important environmental consequence of ground-water overdraft. It is caused by compression of underground materials due to declining water tables or piezometric surfaces. In addition, initiation or acceleration of lateral flow of ground water can cause lateral compression of the aquifer and, hence, lateral movement of the land surface, due to an increase in the seepage force or frictional drag exerted by the flowing water on the solid particles. Theoretically, any flow or overdraft of ground water in unconsolidated material should produce some movement of the land surface. This movement normally is quite small, but it can become significant where underground materials are thick and/or compressible and ground-water levels decline appreciably. Recorded subsidences range from a few centimeters (about 1 inch) to almost 10 m (33 ft), as shown in Table 1. Subsidence rates range from about 1 to 50 cm per 10-m drop in ground-water level (0.01 to 0.5 ft per 10-ft drop), depending on thickness and compressibility of the formations. Lateral movement of the land surface of several meters has been reported in conjunction with removal of oil and gas. Nonuniform subsidence, which may result from different rates of ground-water declines or from differences in compressibility of underground formations, can also produce cracks or fissures in the earth's surface.

Land subsidence has increased flood hazards (Venice, Baytown-Houston) and has caused cracking of buildings, misalignment of bridge abutments, damage to roads, railways, storm sewers or other underground pipelines, collapse of well casings, and reversal of gradients of irrigation canals or other conduits. Land subsidence due to ground-water overdraft is essentially irreversible. It can be stopped by halting declines in ground-water levels (combined with ground-water replenishment if necessary to prevent residual compression of clay layers). However, rebound of the land surface normally is insignificant, even if ground-water levels are restored to presubsidence heights.

INTERGRANULAR PRESSURE

The basic cause of subsidence and lateral movement of the land surface is an increase in the intergranular pressure of the underground materials.

[a]Contribution from the Agricultural Research Service, U.S. Department of Agriculture.

[b]Director, U.S. Water Conservation Laboratory, 4331 E. Broadway, Phoenix, AZ 85040.

Discussion open until February 1, 1978.

Table 1. Examples of Land Subsidence (1 m = 3.28 feet)

	Location	Maximum Subsidence, m	Period	Source
Municipal and Industrial:	Venice, Italy	0.15	1930-1973	Gambolati and Freeze, 1973
	Mexico City	8	1938-1968	Poland, 1969
	Tokyo, Osaka	4	1928-1943	Poland, 1969
	Taipei	1		Poland, 1969
	London	0.18	1865-1931	Poland and Davis, 1969
	Baton Rouge, La.	0.3	Since 1890	Davis and Rollo, 1969
	Houston-Baytown	2.7		Jones and Warren, 1976
Irrigation:	San Joaquin Valley, Calif.	8.5		Lofgren, 1969
	Santa Clara Valley, Calif.	4		Poland, 1969
	Eloy Area, Arizona	2.3	1948-1967	Schumann and Poland, 1969
Geothermal:	Wairakei, New Zealand	4		Axtmann, 1975
Oil:	Wilmington, Calif.	9*		Grant, 1954 Mayuga and Allen, 1969

* In addition, lateral displacements up to 3.7 m were observed.

Such an increase causes a vertical and/or lateral compression of underground formations. The intergranular or effective pressure is the pressure that is transmitted by the individual grains of the underground material at their contact points. For tectonically relaxed systems, the vertical intergranular pressure is defined as

$$P_i = P_t - P_h \qquad (1)$$

where P_i = intergranular pressure,

P_t = total pressure, and

P_h = hydraulic pressure.

This relation can readily be visualized by assuming an imaginary horizontal plane at some depth in the aquifer. The vertical load on this plane is the weight of everything that is above it. However, there is also an upward force acting on the plane, due to the hydraulic pressure of the ground water. The difference between the two loads is the net load, which must be carried by the individual grains of the material.

The total pressure at a given depth is calculated as the weight per unit of horizontal area of everything (solids as well as liquids) that lies above that depth. For the unconfined aquifer in Figure 1 with physical properties as shown in Table 2, for example it can be calculated that P_t at the initial water table is 3.84 kg/cm² (54.6 pounds per square inch, or psi), while at the bottom of the aquifer P_t is equal to 3.84 + 16.96 = 20.8 kg/cm² (296 psi). This yields the P_{t1}-line in Figure 1. The hydraulic pressure increases linearly from zero at the water table to 8 kg/cm² (114 psi) at the bottom of the aquifer, yielding the P_{h1}-line in Figure 1. Above the water table, P_h is negative. Actual values of P_h in this region, however, are difficult to predict because they depend on vertical flow rates and water contents in the vadose zone. For this reason, P_h above the water table normally is considered zero.

The horizontal distance between the P_{t1}-line and P_{h1}-line in Figure 1 is equal to P_{i1}, in accordance with Equation (1). Assuming that the water table has dropped from a depth of 20 m to

Table 2. Physical Properties of Material in Vadose Zone and Aquifer for System in Figure 1 (1 g/cm³ = 62.4 pounds/ft³)

	Porosity %	Volumetric Water Content %	Density of Solids g/cm³	Total Weight g/cm³
Vadose Zone	30	10	2.6	1.92
Aquifer	30	30	2.6	2.12

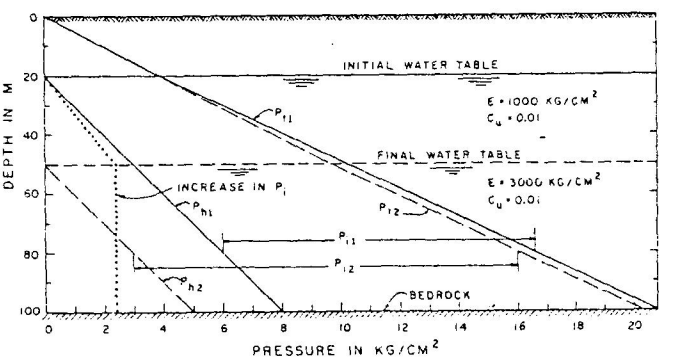

Fig. 1. Effect of water-table drop on total, hydraulic, and intergranular pressure in unconfined aquifer.

50 m (65.6 to 164 ft) and that the water content of the dewatered zone is 10%, like in the original vadose zone, P_t and P_h after the water-table drop can be calculated similarly, yielding the P_{t2}- and P_{h2}-curves indicated with dashed lines in Figure 1. The horizontal distance between the dashed lines is greater than that between the solid lines, indicating that the water-table drop has caused an increase in P_i. At 80-m (262.4-ft) depth, for example, P_i has increased from 10.6 to 13 kg/cm² (151 to 185 psi). The increase in P_i is uniform at 2.4 kg/cm² (34.1 psi) for the entire aquifer below the new water table, but it increases linearly in the dewatered zone from zero at the old water table to 2.4 kg/cm² at the new water table (dotted line in Figure 1).

The increase in P_i is due to the loss of buoyancy of the solids in the dewatered zone (from 20- to 50-m depth). Since the porosity of the material was taken as 30% (Table 2), 1 cm³ of the material contains 0.7 cm³ solids, which upon loss of buoyancy become 0.7 g heavier. Adding the weight of the water remaining behind in the dewatered zone, which at the 10% water content amounts to 0.1 g/cm³, to the weight increase due to loss of buoyancy yields a total effective weight increase of 0.8 g/cm³ of the material in the dewatered zone. Since the dewatered zone is 30 m thick, this amounts to a total weight increase of 2.4 kg/cm², which is the same as the increase in P_i calculated from the P_t- and P_h-lines before and after the water table drop. Thus, for unconfined aquifers, subsidence is caused by compaction of underground materials due to an increase in intergranular pressures resulting from the loss of buoyancy of solids in the zone dewatered by the declining water table.

For confined aquifers, increases in intergranular pressures are caused by decreases in the upward hydraulic pressure against the bottom of the upper confining layer, due to a declining piezometric surface. The decrease in upward hydraulic pressure then effectively causes an increase in the overburden weight. This is illustrated in Figure 2, which shows that the increase in P_i is constant with depth in the aquifer and equal to the reduction in hydraulic pressure due to the drop in piezometric surface. If the upper confining layer contains water in a continuous matrix and there is no ground water above the confining layer, the increase in P_i in that layer will decrease linearly from the aquifer value at the bottom to zero at the top (Figure 2). The values of P_i in Figure 2 were calculated on the assumption that the confined aquifer and the

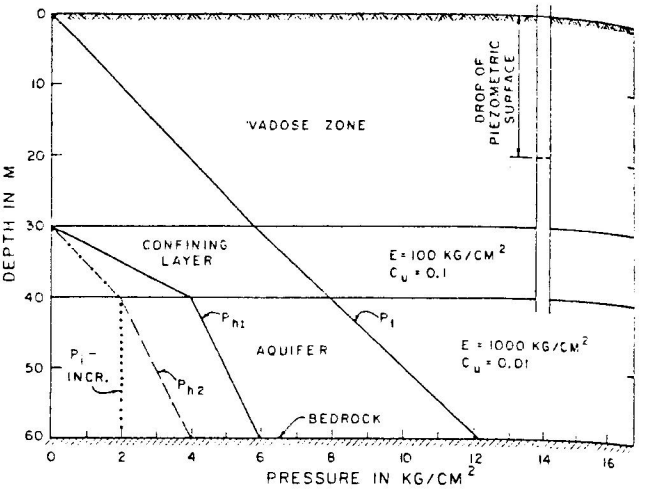

Fig. 2. Effect of drop of piezometric surface on total, hydraulic, and intergranular pressure in confined aquifer.

upper confining layer had the same physical properties as the unconfined aquifer in Table 2, and that the vadose zone had the same properties as shown in Table 2. Since there is no dewatering of pore space by a drop in piezometric surface, the P_t-line is not affected.

CALCULATION OF SUBSIDENCE

The calculation of compression of layers in which P_i is increased is based on how the porosity, or rather the void ratio as commonly used in soil mechanics, of the layer is reduced by an increase in P_i. The relation between void ratio and P_i of a certain unconsolidated material can be determined in the laboratory, by applying increasing vertical loads to a sample and determining the resulting decrease in void ratio from measurements of the compaction of the sample with an extensometer. Curves of the void ratio e versus P_i (Figure 3) generally show that the rate of decrease in e diminishes with increasing P_i. Also, removal of the load causes some rebound of the material, but not to the original position (point A in Figure 3). Resumption of the load produces hysteresis in the curve and when the curve joins the original curve where the load was interrupted, a discontinuity may be observed (point B in Figure 3).

The relation between the compression S_u of a certain layer of thickness Z_1 due to a reduction in void ratio from e_1 to e_2 in conjunction with an effective pressure increase from P_{i1} to P_{i2} can be derived as (see, for example, Bouwer, 1978)

$$S_u = Z_1 \frac{e_1 - e_2}{e_1 + 1} \qquad (2)$$

To calculate subsidence of the land surface, Equation (2) is applied to the various formations

in which P_i is increased. The resulting values of S_u are then summed to obtain the total compression, which is the land subsidence. The value of S_u in response to an increase in P_i can be calculated in two ways: using the elastic theory or the logarithmic theory.

With the elastic theory, the ratio of the stress increase $P_{i2} - P_{i1}$ to the strain or compaction per unit thickness of the layer S_u/Z_1 is considered constant and equal to the modulus of elasticity E. In formula,

$$\frac{P_{i2} - P_{i1}}{S_u/Z_1} = E \qquad (3)$$

Solving this equation for S_u yields

$$S_u = (P_{i2} - P_{i1})\, Z_1/E \qquad (4)$$

which shows how S_u is calculated from the increase in P_i in a layer with thickness Z_1 and an elasticity coefficient of E.

The modulus of elasticity can be evaluated from curves of e versus P_i. Combining Equations (2) and (3) shows that

$$E = \frac{e_1 + 1}{(e_1 - e_2)/(P_{i2} - P_{i1})} \qquad (5)$$

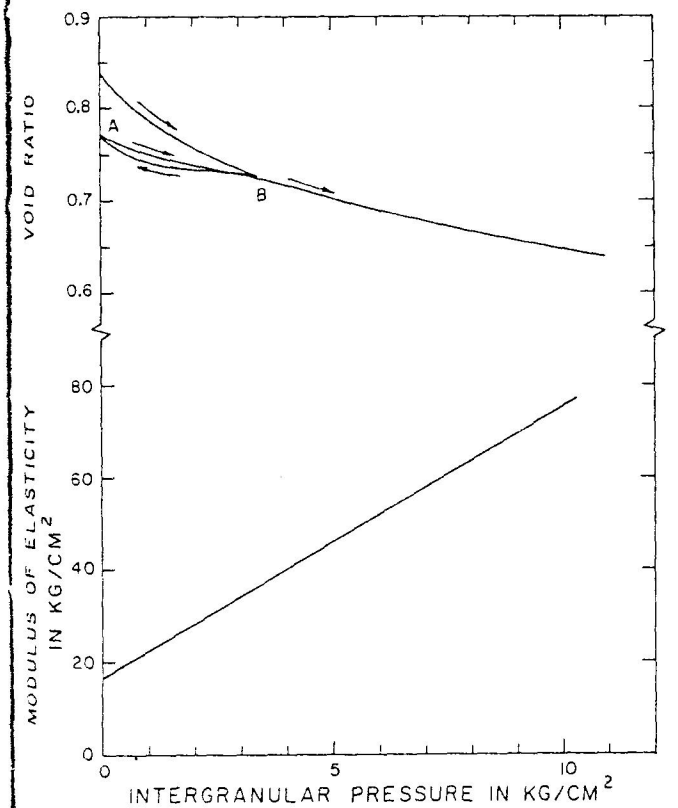

Fig. 3. Hypothetical relation between void ratio and intergranular pressure for medium-textured material (top) and resulting relation between modulus of elasticity and intergranular pressure (bottom).

which can also be written as

$$E = \frac{e + 1}{de/dP_i} \qquad (6)$$

where de/dP_i is the slope of the curve of e versus P_i. These slopes can be graphically determined from experimental curves. For true elastic materials, E is constant. For soils and aquifer materials, however E tends to increase with increasing P_i. This is illustrated by the E-curve in Figure 3, which was calculated by determining the slope of the e curve in this Figure for various values of P_i (ignoring the rebound curve and the first segment of the recompression curve), and calculating E with Equation (6). The increase in E with increasing P_i means that E for a uniform layer will increase with depth, because P_i increases with depth. To calculate S_u for such a formation, the layer is divided into a number of small depth increments, each with its own values of P_i and E. The compaction of each increment is calculated with Equation (6). The resulting values are then summed to give the compression of the entire formation. Sometimes the reciprocal of E, called the compressibility index, is used in subsidence calculations (Gambolat *et al.*, 1974).

The dependency of E on P_i is avoided with the logarithmic theory by Terzaghi (see, for example, Terzaghi and Peck, 1948). This theory is based on the fact that when e is plotted against log P_i, a sigmoid curve is generally obtained with flat portions for the very low and very high values of P_i, but with an essentially straight section for the mid-range of P_i-values. The slope of this linear section is called the compression index C_c and is calculated as

$$C_c = \frac{e_1 - e_2}{\log P_{i2} - \log P_{i1}} \qquad (7)$$

Solving this equation for $e_1 - e_2$ and substituting the result into Equation (2) then yields

$$S_u = Z_1 \frac{C_c}{e_1 + 1} \log \frac{P_{i2}}{P_{i1}} \qquad (8)$$

This equation is, of course, valid only for the P_i-range where e varies linearly with log P_i. Values of e_1 usually range between 0.7 and 1.3. Thus, $e_1 + 1$ varies from about 1.7 to 2.3. This is a variation of only 15% from the average value of 2. Since the uncertainty in C_c probably will be more than 15% (particularly when applying laboratory data to field conditions), the term $C_c/(e_1 + 1)$ in Equation (8) can be combined into one compression

Table 3. Orders of Magnitude of E (1 kg/cm² = 14.2 psi) and C_u (dimensionless) for Unconsolidated Materials (as Compiled from Various Sources by Bouwer, 1978)

	E in kg/cm²	C_u
Dense gravel and sand	2,000-10,000	0.005
Dense sand	500-2,000	0.01
Loose sand	100-200	0.05
Dense clay and silt	100-1,000	0.05
Medium clay and silt	50-100	0.1
Loose clay	10-50	0.3
Peat	1-5	0.2-0.8

coefficient C_u (see, for example, Colijn and Potma, 1944), reducing Equation (8) to

$$S_u = Z_1 \, C_u \log \frac{P_{i2}}{P_{i1}} \qquad (9)$$

To apply Equation (4) or Equation (9), one must know E or C_u. These coefficients can be evaluated from laboratory tests as discussed earlier, or they can be determined from measured subsidence or compression in response to a certain drop of water table or piezometric surface. Approximate ranges for E and C_u are listed in Table 3. These values should be considered only as general ones and should not be used to predict subsidence for actual situations. Such predictions should be based on local values of E or C_u. The data in Table 3 show that the compressibility of granular materials increases with decreasing particle size. Organic deposits are the most compressible. By way of comparison, E of water is about 20,000 kg/cm² (284,460 psi).

Examples of Using Equations (4) and (9)

Assuming that the unconfined aquifer in Figure 1 consists of dense sand with E = 1,000 kg/cm² for the dewatered zone from 20 to 50 m and E = 3,000 kg/cm² for the lower 50 m of the aquifer (the higher value of E accounts for the fact that E increases with increasing P_{i1}) and taking the average P_{i1}- and P_{i2}-values for each zone, Equation (4) yields S_u = 0.036 m for the 20- to 50-m zone and S_u = 0.024 m for the 50- to 100-m zone, or a total subsidence of 0.06 m. Taking C_u = 0.01 for both zones (the logarithmic theory automatically takes care of the decreasing compressibility of the material with increasing depth), Equation (9) yields S_u = 0.026 m for the 20- to 50-m zone and 0.028 m for the 50- to 100-m zone, or a total subsidence of 0.054 m. Thus, the subsidence is about 2 cm per 10-m water-table drop. This is at the low end of the range observed in practice, as can be expected for an aquifer consisting of dense sand with no clay layers. If the aquifer below the 50-m depth in the example had contained beds of compressible clay with a total thickness of 20 m and an E-value of 30 kg/cm², the compression due to a P_i-increase of 2.4 kg/cm² would have been 1.6 m. The resulting subsidence from the clay layers alone thus would have produced a subsidence of 0.53 m per 10-m water-table drop, which is at the top of the range of values observed in practice.

For the confined aquifer in Figure 2, taking E as 100 kg/cm² for the upper confining layer (clay) and as 1,000 kg/cm² for the aquifer (sand) and again using the average P_i-values for each layer, Equation (4) yields S_u = 0.1 m for the confining layer and S_u = 0.04 m for the aquifer. Taking C_u as 0.1 for the confining layer and 0.01 for the aquifer, Equation (9) yields S_u-values of 0.082 and 0.029 m, respectively. Thus the total subsidence is 0.14 and 0.112 m, respectively, for these solutions, which yields a subsidence of about 0.06 m per 10-m drop in piezometric surface. If compression of the aquifer and of the upper confining layer is the only way in which water is yielded, the storage coefficient of the aquifer would be 0.006. Since E for water (i.e., 20,000 kg/cm²) is several orders of magnitude higher than E for unconsolidated materials, expansion of water contributes insignificantly to storage coefficients of confined aquifers consisting of such materials. Only when the water is saturated with certain dissolved gases which go out of solution upon pressure reduction, will decompression of water contribute significantly to storage coefficients.

The treatment of subsidence in this paper is a simple and elementary way of predicting final subsidence due to ground-water overdraft. Actually, the subsidence rate may lag behind the ground-water decline rate, because it may take time for water to be squeezed out of clay layers being compressed. If the clay is tight and the layers are thick, decades may pass before the excess pore water has been released and the increase in effective overburden pressure is entirely carried by the clay particles at their contact points. In such cases, subsidence can continue many years after ground-water decline has stopped. Such residual subsidence can be avoided by restoring ground-water levels to original elevations. The rate of compression of a clay layer in response to a load increase varies linearly with the hydraulic conductivity of the layer and inversely with the square of the thickness of the layer (Terzaghi and Peck, 1948).

Fig. 4. Ero
southeast

Unc
draft and
the land
be simpl
lateral of
reported
Arizona
probably
1 or 2 ki
concentr
basin an
surround
the surfa
intercep
intercor
eventua
5 to 10
(6 miles
have be
33 ft) d
soil ma
portion
second
drilling
R. H. I
Phoeni

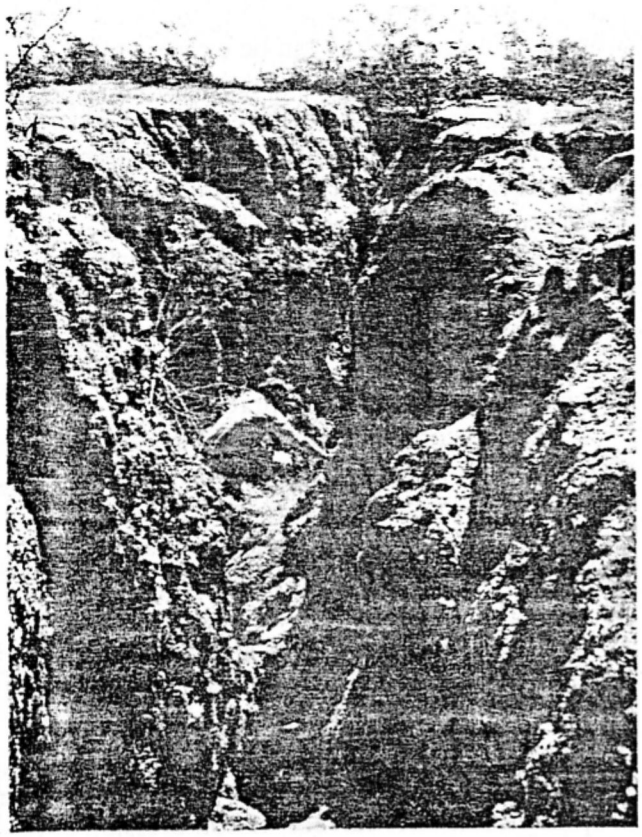

Fig. 4. Eroded earth crack in caliche-cemented alluvium southeast of Chandler, Arizona.

CRACK FORMATION

Under certain conditions, ground-water overdraft and resulting subsidence can cause fissures in the land surface. Most of these cracks appear to be simple tensional breaks with no vertical or lateral offset. Schumann and Poland (1969) reported for a ground-water basin in south-central Arizona that such cracks initially were narrow, probably less than 2 cm (0.8 in.) wide and about 1 or 2 km (1 mile) long. The cracks appeared to be concentrated along the periphery of the subsiding basin and ran approximately parallel to the surrounding mountains. Most cracks ran normal to the surface-drainage pattern, causing them to intercept runoff, erode, cave, and become interconnected. Some of the resulting "gullies" eventually were several meters (about 10 ft) wide, 5 to 10 m (16 to 33 ft) deep, and more than 10 km (6 miles) long (Figure 4). The cracks initially may have been deeper than their final 5- to 10-m (16 to 33 ft) depth, because caving and accumulation of soil material may have filled or covered the deeper portions. Vertical extension of cracks below the secondary fill has been observed by excavation and drilling in the fissures (personal communication, R. H. Raymond, U.S. Bureau of Reclamation, Phoenix, Arizona). Schumann and Poland also reported that the trends of several of the fissures conformed with linear zones of steep gravity gradients adjacent to mountain ranges. These steep gradients may indicate buried fault scarps.

Formation of tensile cracks above buried fault scarps at the periphery of a subsiding basin could be the result of a linearly increasing subsidence from the edge of the basin to the center. Such increasing subsidence then could produce a rotational movement of the upper slab of alluvial fill around the top of the underground scarp (Figure 5). An approximately linear increase in subsidence from the edge of the basin to the center can be caused by greater withdrawal of ground water in the center portion of the basin. Also, deep clay beds and other compressible formations may be thickest in the center of the basin and become thinner towards the edges. Under these conditions, compression of the deeper clay beds and other materials below the water table tends to increase from the edge of the basin to the center, causing the overlying alluvium to rotate from CE to CF above the compressing layers and from AB to AD at the surface, and a crack to be formed above the scarp (Figure 5). The pivot point for the rotation is where the compressible deposits in Figure 5 run out against the underground scarp. If there is no compression at that point, the fissure will be a simple, tensional break. The same will be true if compressible layers on both sides of the scarp undergo equal compression. If, however, compression takes place on the basin side of the underground scarp but not on the mountain side, the fissure may also show a vertical offset. Assuming that AB in Figure 5 is about 10 km (6 miles), BD is 2 m (6.6 ft) and AC is 50 m (164 ft), application of similar triangles to the crack and triangle ABD shows that initially the crack is 1 cm (0.4 inch) wide at the surface, which is on the same order as observed in the field (Schumann and Poland, 1969).

The rotating-slab theory may also explain

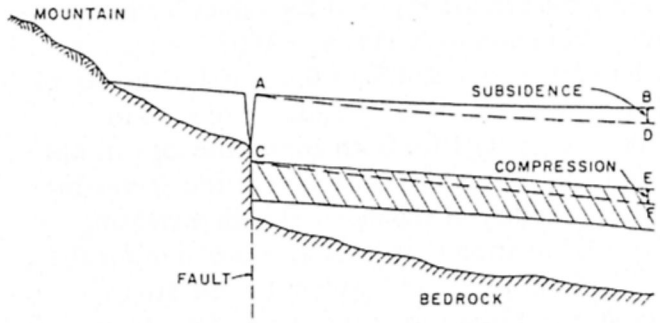

Fig. 5. Schematic of crack development above buried scarp due to rotation of slab ABEC.

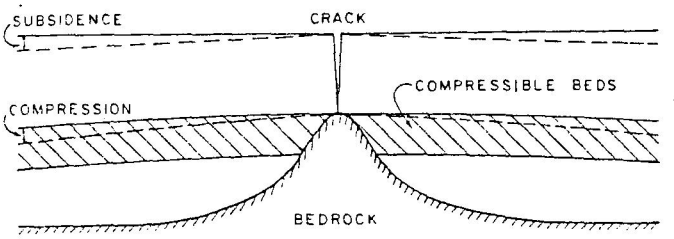

Fig. 6. Schematic of crack development above bedrock ridge.

formation of cracks above underground ridges in basement rock (Figure 6). Since the areas above such ridges tend to be less suitable for well sites because of the limited depth, ground-water withdrawal tends to be concentrated at some distance on both sides of the ridge where the alluvial materials are thicker. This could produce a linearly increasing subsidence away from the ridge, causing the overlying slabs on each side of the ridge to rotate similar to the rotation in Figure 5, and cracks to form above the ridge.

It may also seem plausible that earth cracks could be formed by a stretching of the land surface. If the subsidence is purely vertical, AD in Figure 5 is longer than AB. However, this normally gives such a narrow crack [0.2 mm (0.008 inch) if AB = 10 km (6 miles) and BD = 2 m (6.6 ft)], that it is not a likely explanation. Another possible reason for crack formation is differential lateral movement of the land surface. If ground-water withdrawal is concentrated in a certain part of a ground-water basin, lateral flow rates of ground water will be highest in and near that area. Because of horizontal seepage forces, this will then produce more lateral compression, and, hence, more lateral movement of the land surface near the area of pumping than at some distance away. The differential lateral movement then could produce cracks that may run more or less concentric in or around the area of pumping. Cracks could also be concentrated where there are discontinuities in underground materials, such as alluvial fans with coarse-textured materials and little tensile strength grading into finer, more plastic valley fills. Another possible mechanism for crack formation, proposed by Holzer (1976), is differential lateral movement by horizontal shrinkage of the sediments in the zone dewatered by declining ground-water levels.

Earth cracking is a surface manifestation of ground-water overdraft that can be caused by a variety of subsurface conditions that sometimes may be quite complex. While the models and mechanisms presented in the previous paragraphs may give some of the reasons for earth cracking, true causes can only be evaluated by intensive field and subsurface investigations. Considering the increased use of ground water and the potential damage of land subsidence and particularly earth cracking due to ground-water overdraft, additional research to determine causes and to predict where earth cracks may develop is very much needed.

REFERENCES

Axtmann, R. C. 1975. Environmental impact of a geothermal power plant. Science. v. 187, pp. 795-803.

Bouwer, Herman. 1978. Groundwater hydrology. McGraw-Hill Book Company, New York, N.Y. (in press, scheduled for 1978).

Colijn, P. J., and J. Potma. 1944. Weg-en Waterbouwkunde. I. Grondmechanica. Kosmos, Amsterdam.

Davis, G. H., and J. R. Rollo. 1969. Land subsidence related to decline of artesian head at Baton Rouge, Lower Mississippi Valley, U.S.A. Proc. Tokyo Symp. on Land Subsidence, IASH-UNESCO, pp. 174-184.

Gambolati, G., and R. A. Freeze. 1973. Mathematical simulation of the subsidence of Venice. 1. Theory. Water Resources Research. v. 9, pp. 721-733.

Gambolati, G., P. Gatto, and R. A. Freeze. 1974. Mathematical simulation of the subsidence of Venice. 2. Results. Water Resources Research. v. 10, pp. 563-577.

Grant, U. S. 1954. Subsidence of the Wilmington oil field, California. *In* Geol. of Southern California, R. H. Johns, ed., Calif. Div. Mines Bull. 170, Chapter 10, pp. 19-24.

Holzer, R. L. 1976. Ground failure in areas of subsidence due to ground-water decline in the United States. Proc. 2nd Internat. Symp. on Land Subsidence, Internat. Assoc. Sci. Hydrol., Anaheim, Calif., Dec. 13-17.

Jones, L. L., and J. P. Warren. 1976. Land subsidence costs in the Houston-Baytown area of Texas. Jour. Amer. Water Works Assoc. v. 68, pp. 597-599.

Lofgren, B. E. 1969. Field measurement of aquifer-system compaction, San Joaquin Valley, California, U.S.A. Proc. Tokyo Symp. on Land Subsidence, IASH-UNESCO, pp. 272-284.

Mayuga, M. N. and D. R. Allen. 1969. Subsidence in the Wilmington oil field, Long Beach, California, U.S.A. Proc. Tokyo Symp. on Land Subsidence, IASH-UNESCO, pp. 66-79.

Poland, J. F. 1969. Status of present knowledge and needs for additional research on compaction of aquifer systems. Proc. Tokyo Symp. on Land Subsidence, IASH-UNESCO, pp. 11-21.

Poland, J. F., and G. H. Davis. 1969. Land subsidence due to the withdrawal of fluids. Reviews in Engineering Geology II, Geol. Soc. Amer., Boulder, Colorado, pp. 187-269.

Schumann, H. H., and J. F. Poland. 1969. Land subsidence, earth fissures, and groundwater withdrawal in south-central Arizona, U.S.A. Proc. Tokyo Symp. on Land Subsidence, IASH-UNESCO, pp. 295-302.

Terzaghi, K., and R. B. Peck. 1948. Soil mechanics in engineering practice. John Wiley & Sons, Inc., New York, N.Y.

Attenu
Throu

by C. W. Fett

Seconda
columns filled
period of 10 w
was retained i
primarily due
nitrogen were
There was no
and it was pre
About 30 per
exchange in t
probably due
sites.

Physi
soil are kn
transform
refractory.
combined
waste-wat
High-rate
seepage b
recharge a
waste-wat
1974).

The
fate of ni
containec
into seep

[a]As
Wisconsin
Dis